Global NEST Journal, Vol 25, No 6, pp 1-11

Prediction of land use and landcover changes in Tiruppur Tamilnadu using hybrid convolutional neural network

Akshaya K.G.[a,*] and Sathyanarayan Sridhar R.[b]
[a]Easwari Engineering College, Ramapuram, Chennai, Tamil Nadu 600089, India
[b]Coimbatore Institute of Technology, Coimbatore, Tamil Nadu 641014, India
Received: 02/01/2023, Accepted: 18/02/2023, Available online: 22/03/2023
*to whom all correspondence should be addressed: e-mail: akshaya.kg.civil@gmail.com
https://doi.org/10.30955/gnj.004716

Graphical abstract

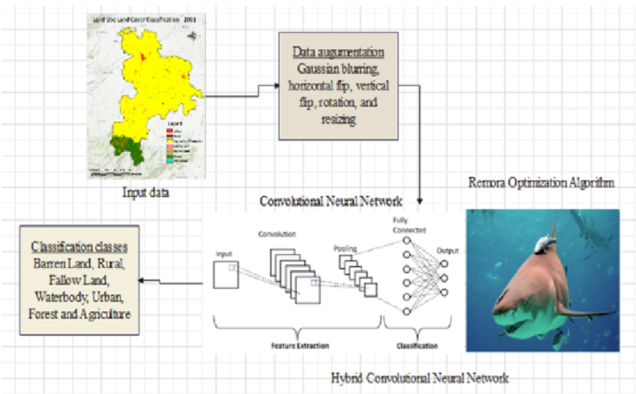

Abstract

Land use and land cover change (LU/LC) are important in global change studies because they can transform the local and global environment by developing the biochemical, biochemical, and biogeographic properties of the Earth's structure. This paper is intended to develop Hybrid Convolutional Neural Network (HCNN) for land use and land cover changes prediction in Tiruppur Tamilnadu. Initially, the databases are collected from the open-source system. And the image dataset has been pre-processed using the image augmentation technique. Through which the image has been resized and processed for training with the proposed mode. The resized images are sent to the HCNN for prediction of land cover and land use changes in Tiruppur Tamilnadu. The proposed classifier is a combination of Convolutional Neural Network (CNN) and Remora Optimization Algorithm (ROA). In the CNN, the ROA is utilized to select the hyperparameters to enable efficient prediction in land use and land cover changes. The proposed classifier is implemented in MATLAB and performances are evaluated by performance metrics such as accuracy, precision, recall, sensitivity, F_Measure, and Kappa. The proposed methodology is compared with conventional techniques such as CNN, Markov chain model, and Recurrent Neural Network (RNN) respectively.

Keywords: Hybrid convolutional neural network, remora optimization algorithm, performance metrics, Markov chain, and deep learning

1. Introduction

Urban landscapes are a way of life that is constantly undergoing dynamic changes. They are affected by the qualities and behavior of the people living nearby. All types of land-mediated human mediation to address the issues of human existence truly and deeply can be considered phenomena of LU/LC change (Souza *et al.*, 2020) LU/LC changes are an inevitable consequence of progress. Most often, these improvements occur due to population growth and a longing for higher personal satisfaction (Mansour *et al.*, 2020). These developments are further affected by a combination of natural, geographical, and financial variables and institutional and strategic factors. There are multiple complementary relationships with critique between the effects of LU/LC changes and driving components (Cegielska *et al.*, 2018). These collaborations can affect small and large-scale financial structures, cause changes in the public action arrangement of the local area, and affect the climate of the district (e.g., environmental change and range of reporting) (Hussain *et al.*, 2020).

A few researchers focusing on LU/LC change have focused on the selection of driving variables, for example, population thickness, distance from the street, distance from the waterway, distance from the nearest town (Namugize *et al.*, 2018), distance from the city center (downtown area), a region already developed, current countryside Distance, distance from passenger locations (financial variables), and biophysical factors (elevation, slope, rock, soil type). Similarly, the factors that drive LU/LC changes at specific levels include natural variables (Berihun *et al.*, 2019) (e.g., temperature and rainfall), financial components (e.g., GDP), the presence and inclination of protected areas, and authoritative perspectives and attitudes (Hamad *et al.*, 2018). Analysts and leaders face difficulties in studying complex true peculiarities such as LU/LC transformation. One of the most commonly taken strategic approaches is to fix the problem without losing the central object, for example, by building models to address the key areas that drive uniqueness (Nayak and Mandal, 2018). The uniqueness of the LU / LC change can be demonstrated by different techniques and adjusted to the desired results (results).

GIS and remote sensing methods have been extensively employed in studies on changes in land use and land cover (LU/LC). These methods make it possible for this study to reliably and efficiently gather and evaluate vast volumes of geographic data. To monitor changes in land use and land cover over time, for instance, remote sensing data may be used to create maps of land cover at various geographical and temporal scales. To better understand the variables influencing LU/LC change, GIS software may be used to analyze, display, and combine this data with other kinds of data (such as demographic, economic, and environmental data). To create models that can forecast future land use and land cover patterns based on past trends and other variables, GIS and remote sensing methods have also been applied.

The loss function creates a numerical number that indicates the difference between the real output and the model's anticipated output as inputs. The model's ability to anticipate the right output is improved with decreasing loss. The model modifies the weights and biases of its internal parameters to decrease the error between the expected and true output to minimize the loss during training. This is often accomplished by repeatedly adjusting the model's parameters to decrease loss using an optimization procedure, such as stochastic gradient descent.

The image dataset in this study has been pre-processed using the image augmentation technique. Image augmentation is a method of artificially increasing the size of a dataset by generating modified versions of existing images. This can be done by applying various transformations to the images such as cropping, rotating, scaling, flipping, and adding noise. The goal of image augmentation is to create a larger, more diverse dataset that can be used to train machine learning models. This can help to improve the generalizability and robustness of the model, as it has been trained on a wider range of image variations.

The role of the Remora Optimization Algorithm (ROA) in the Hybrid Convolutional Neural Network (HCNN) is to assist in the selection of hyperparameters that can improve the efficiency of the classifier for predicting land use and land cover changes. Hyperparameters are settings that are chosen by the designer of a machine learning model and are not learned from the data during training. They can have a significant impact on the performance of a model and must be carefully chosen to achieve good results. The ROA is an optimization algorithm that is used to search for the optimal values of the hyperparameters in the HCNN. By optimizing these values, the ROA aims to improve the performance of the HCNN for the task of predicting land use and land cover changes.

Many factors can contribute to land use and land cover (LU/LC) change including;

Demographic factors: Changes in population size, age structure, and population growth rate can affect land use and land cover patterns. Population growth may lead to an increase in the demand for housing and urban development, resulting in changes in land cover.

Economic factors: The expansion of commercial and industrial activities may lead to the conversion of natural areas to developed land.

Environmental factors: Changes in climate, weather patterns, and natural disasters can also affect land use and land cover.

Political and policy factors: Land use and land cover patterns can also be influenced by zoning laws and land use planning policies can regulate the type and location of the development, impacting land cover patterns.

Technological factors: The development of new agricultural techniques may lead to the conversion of natural areas to cropland, or the use of new transportation technologies may facilitate urban sprawl.

Land use and land cover (LU/LC) changes can have a range of impacts on local and global environments including; the loss of natural habitats, which can lead to the extinction of plant and animal species. This can have negative impacts on local ecosystems and the overall biodiversity of an area. Climate change: this affects the carbon cycle, leading to changes in the number of greenhouse gases in the atmosphere. For example, the conversion of natural areas to developed land can release carbon stored in vegetation and soil, contributing to global warming. LU/LC can also impact water quality, as the type and amount of land cover can affect the amount of runoff and the number of pollutants that enter waterways. LU/LC have indirect impacts on human health, as they can alter the availability and quality of natural resources such as water and timber, and can affect the quality of the environment in which people live.

The HCNN used in this study combines elements of a Convolutional Neural Network (CNN) with the Remora Optimization Algorithm (ROA) to make predictions about land cover and land use changes in Tiruppur Tamilnadu. The HCNN is trained using the processed images and is intended to accurately predict changes in land use and land cover in the study area.

The performance of the HCNN model is evaluated using a variety of metrics, such as accuracy, precision, recall, and F-measure, which are typically calculated based on the number of correct and incorrect predictions made by the model. Other metrics, such as error rate and kappa, are also used to evaluate the performance of a model.

The main contribution of the research on land use and land cover (LU/LC) change prediction involves the development of a novel method of combination of Convolutional Neural Network (CNN) and Remora Optimization Algorithm (ROA) for predicting LU/LC changes, or the demonstration of the effectiveness of a particular approach or technique in this domain. Alternatively, the research contributes new insights or understanding about the factors that contribute to LU/LC change or the impacts of such changes on local or global environments.

GIS discovery and remote sensing have been used in research on endless suburbs, soil erosion, LU / LC, avalanche, wellness risk, land equity, agricultural land structure, water use efficiency, NDVI, and more. In particular, remote detection and GIS detection are widely used in conjunction with neural network technology (Choudhury *et al.*, 2019). This strategy is animated by a numerical display of nerves in the human cerebellum. In many types of brain systems, the Feedforward Neural Network (FNN) is a basic and time-consuming technique (Khamchiangta and Dhakal, 2020). There are two types of FNN techniques: single-layer perceptron (SLP) and multi-layer perceptron (MLP). In recent years, the deep learning-based Convolutional Neural Network (CNN) is considered to empower prediction accuracy. The main contribution of the work is presented as follows,

- This paper is intended to develop HCNN for land use and land cover changes prediction in Tiruppur Tamilnadu. Initially, the databases are collected from the open-source system. And the image dataset has been pre-processed using the image augmentation technique.
- Through which the image has been resized and processed for training with the proposed mode. The resized images are sent to the HCNN for prediction of land cover and land use changes in Tiruppur Tamilnadu.
- The proposed classifier is a combination of CNN and ROA. In the CNN, the ROA is utilized to select the hyperparameters to enable efficient prediction in land use and land cover changes.

The extra portion of the paper is pre-planned as follows, section 2 gives the related work review of the land use and land cover changes. The projected approach is explained in section 3. The outcomes are explained in portion 4. The summary of the paper is presented in section 5.

2. Related works

Xiaoming Xu *et al.* (2020) have studied the dynamics and drivers of land use and landscape change in Bangladesh. Here, the drivers of the major LU/LC were measured by mixing with biophysical and financial sensitivities at the subdivision level. Here, Landsat used satellite data to understand LU/LC from 2000 to 2010 and used a global surface water database to indicate the effects of water anomalies. The results suggest that large LU/LC horticultural land and water bodies in Bangladesh will occur between forests and shrublands. Occasional water rejection will work on the accuracy of our LU/LC results and driving test. Although the net accumulation and loss of agricultural land were large in the vicinity, the net conversion (narrow increase in net total deficit) was practically small at the national level. Environmental factors and changes in outbreaks and circumstances and in urban and country families are driving the progress from forest to shrubland in the southeastern district.

Andi Muhammad Yasser Hakim *et al.* (2021) have presented a multi-layer perceptron neural network (MLPNN) to demonstrate the expectations of land use/land cover change. The study uses Remote Sensing and Geographic Information System (GIS) tools to provide a forecast model of land use/landscape changes in the city of MacArthur by 2031. This model is based on spot satellite images from 2006, 2011, and 2016. Evaluation of 10 driving variables. The MLPNN strategy was driven by the Markov chain model, which incorporated the business-conventional scenario. The results predict that by 2031, McCormack will cover 80% of the city's total growth.

Abijith Devanantham *et al.* (2021) have presented a Landscaping and Landscaping Authorization and Estimates of Expectations including Remote Detection and CA Markov in the northern coastal areas of Tamil Nadu, India. Concentrated coastal use and topography help to divert change and control climate maintenance. Later, the study breaks the northern TN coast, which is under conventional and anthropological pressure. The investigation of LULC changes and LULC forecasts for the district between 2009-2019 and 2019-2030 was carried out using Google Earth Engine (GEE), TerrSet, and GIS tools. The LULC image was created from Landsat images and compiled in GEE using Random Forest (RF). LULC maps were outlined with the CA-Markov model to measure future LULC transformation.

J. Jagannathan *et al.* (2021) have introduced a deep convolutional neural network of land use and forecasting and characteristics of landscape changes. In this paper, a hybrid hot encoding VGG19 deep learning strategy is proposed. Furthermore, a transfer learning strategy has been used to move product information generated by the RestNet50 technique to the proposed HGVGG19 strategy. Satellite images and aerial images are collected from various sources and sorted in the view of the elements. What's more, the image database was handled in advance using the image enhancement method. This resized the image and manipulated it to produce it in the proposed mode. Clear information cannot be handled directly, so use a hot coding technique to determine class boundaries.

Bhanage Vinayak *et al.* (2021) have introduced the Markov chain model based on a multi-layer perceptron neural network to predict land use and landscape changes in Mumbai. In this review, it was suggested that the forecast for upcoming land use landcover (LULC) changes in Mumbai and its environs should include reference data of metropolitan events. To get the actual elements of LULC, the managed arrangement calculation was used for Landsat films of 1992, 2002, and 2011. In light of spatial drivers and LULC of 1992 and 2002, The Markov Chain Model (MCM) based on the MLPNN was used in 2011 to recreate LULC, which was further approved using kappa measurements. From that point on, MLPNN-MCM was used to anticipate LULC in 2050, using LULC in 2002 and 2011.

Girma, R *et al.* (2022). According to research, it is necessary to apply ecologically friendly management practices to reduce these negative effects of land use change. The results of this research will be beneficial in giving people the chance to create an acceptable plan for protecting land and water resources.

Geng, J *et al.* (2022), combined nonlinear spatiotemporal dependency learning and CA-based spatial allocation to present a hybrid spatiotemporal convolution-based cellular automata model (ST-CA) as a solution to this issue. The model was modified to include a three-dimensional convolutional neural network (3D-CNN) to include both the spatiotemporal dependencies and the nonlinear driving mechanism. It helps create more complex development potentials to boost simulation accuracy.

Mulualem Tegegne, A *et al.* (2022), to perform spatial assessments of groundwater potential zones and land cover. The classification of land cover (agriculture, built-up, water bodies, forests, and bare land) has been reported as one of the factors influencing groundwater for various reasons, and several researchers have approved CNN's capability to predict the spatial groundwater potentiality zones of very high, high, moderate, poor, and very poor areas. For the identification of groundwater potential zones and the categorization of changes to land use and land cover, CNN is suggested as a crucial algorithm in this research.

3. Proposed system model

In recent years, remote sensing technologies are increasingly advanced. Satellite image acquisitions are considered to evaluate remote sensing technologies. The land use and land cover classification in tasks as augmentation and classification. This paper is intended to develop HCNN for land use and land cover changes prediction in Tiruppur Tamilnadu. Initially, the databases are collected from the open-source system. And the image dataset has been pre-processed using the image augmentation technique. Through which the image has been resized and processed for training with the proposed mode. The resized images are sent to the HCNN for prediction of land cover and land use changes in Tiruppur Tamilnadu. The proposed classifier is a combination of CNN and ROA. In the CNN, the ROA is utilized to select the hyperparameters to enable efficient prediction in land use and land cover changes. This dataset is containing different classes such as Barren Land, Rural, Fallow Land, Waterbody, Urban, Forest, and Agriculture. The complete architecture of the projected approach is given in Figure 1.

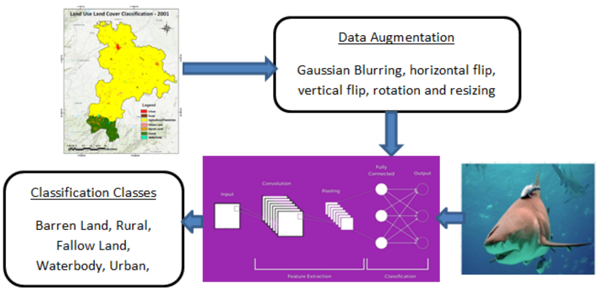

Figure 1. Proposed Architecture

3.1. Data augmentation

The volume and diversity of training data play eminent roles in training an efficient deep-learning model. The general data augmentation technique is utilized to empower the diversity of the data to a different extent through developing visual variability that assists the model to interpret the data with high accuracy. From the considered database, the data augmentation methods are utilized to enhance the accuracy of classification in land use and land cover. In this proposed approach, the different data augmentation techniques are considered such as resizing, rotation, vertical flip, horizontal flip, and gaussian blurring (Naushad *et al.*, 2021).

The volume and diversity of training data play a crucial role in training a deep learning model. In general, the more data that a model is trained on, the better it will perform. This is because more data allows the model to learn more about the patterns and relationships present in the data, enabling it to make more accurate predictions. It is also important for the training data to be diverse, meaning that it covers a wide range of examples and variations within the domain of interest.

3.2. Convolutional neural network

The augmented data is utilized to classify.

The different CNN layers of operation are mathematically presented as follows.

3.2.1. Convolution layer

The operation of convolution for every layer of CNN is presented as follows,

$$CL_F^S(Y)=\varphi\left[\left(\sum_{CH=1}^{CH}\sum_{K=1,X=P}^{K=1,X=P+T}\left(W_f^{CON^s}(K)\times CL_C^{S-1}(X)+B_F^{CON}\right)\right)\right] \quad (1)$$

Here, T can be described as the total parameter of a similar filter, B_F^{CON} can be described as the signifies bias term of the fth filter, $W_f^{CON^s}(K)$ can be described as the weight of the sth layer, the pixel parameter of s-1 th convolutional layer with the specified position of the CL_C^{S-1} (X), here, CL can be described as the total number of channels and S can be described as the initial pixel solution, S−1 can be described as the convolution layer pixel parameter, and filter position is represented as the CL_F^S (Y). In this model of CNN, three convolution layers and a sigmoid transfer function are considered (Kumar *et al.*, 2021).

In this CNN model, there are three convolutional layers. These layers apply a set of filters to the input data, using these filters to detect various features in the data. The number of filters used in each convolutional layer, as well as their size and stride, can be specified by the designer of the model. The output of each convolutional layer is pas through a sigmoid transfer function before being passed on to the next layer. The sigmoid function is a non-linear activation function that maps the input data to a range of 0 to 1. This can help to introduce non-linearity into the model and improve its ability to capture complex patterns in the data. It is worth noting that other activation functions, such as the ReLU function, are often used in CNN's in place of or in addition to the sigmoid function.

3.2.2. Maximum pooling layer

The CNN pooling operation process is formulated as follows,

$$m_C^Y(Y) = MAX\left(L_F^S(X)\right) for\ X = 1,\ \ 1 to Pat_{H,} Pat_W \tag{2}$$

Based on the above equation, Pat_H, can be described as the patch height, Pat_W can be described as the patch width, m_C^Y (Y) can be described as the pixel parameter achieved after the application of higher pooling on the ch[th] channel and s[th] layer.

3.2.3. Fully connected layer

This layer is presented the mathematical procedure that connected with a fully connected layer which is presented as follows,

$$i_{FC} = \varphi\left[\sum_{k=1}^{K}\left(Feat_K \times w_{K,J}^{FC}\right) + B_J^{FC}\right] \tag{3}$$

Where, $Feat_K$ can be described as the feature vector, K can be described as the total input features, i_{FC} can be described as the output of the hidden layer neuron, $w_{k,j}^{FC}$ can be described as the weight of the input feature of the hidden layer.

3.2.4. Softmax layer

The mathematical formulation of the Softmax layer that identifies the output of land use scenarios is presented as the equation (4). In this section, different land use conditions are validated by the projected technique. This layer contains the loss presented while the training stage. The existing cost function (5) can be an objective function that should be reduced to identify the data. The CNN reduces the loss computed by a Softmax layer.

$$P_{so} = \frac{EXP\left(I_{FC}\right)}{\sum_{FC=1}^{FC} EXP\left(I_{FC}\right)} \tag{4}$$

The existing cost function can be presented as follows,

$$E^{Modified} = CE + \beta\sum\omega^2 \tag{5}$$

The fully connected layer is containing the different variables that adhere to deep learning from the small dataset. In this research, a sparsity cost is can be added to the conventional cost function that can generate deep learning. The sparsity can be connected with avoiding unnecessary activation of neurons in the CNN hidden layer of CNN.

The proposed approach uses sparsity to improve deep learning from small datasets by adding a sparsity cost to the conventional cost function of the fully connected layer in the convolutional neural network (CNN). By reducing the number of active neurons in the hidden layer, the model may be able to focus on more relevant features in the data and improve its ability to generalize to new examples.

$$E^{Modified} = CR + \beta\sum\omega^2 + \beta 1\sum_{J=1}^{m} n\left(\mu,\mu_J^t\right) \tag{6}$$

Here,

$$CE = \sum_{J=1}^{m} y_I^t Ln Y_J^P \tag{7}$$

And,

$$n\left(\mu,\mu_J^t\right) = \sum_{J=1}^{J}\left[\begin{array}{l} -6\tan 1 + \left(2+\mu+\mu_J^t\right)tan \\ \left[\dfrac{8+\left(\mu^2+\left(\mu_J^t\right)^2\left(\mu+\mu_J^t\right)^2\right)}{8\left(1+\mu^2+\left(\mu_J^t\right)^2\right)}\right] \\ +\left(4-\mu-\mu_J^t\right)tan \\ \left[\dfrac{8+\left(1-\mu\right)^2+\left(1-\mu_J^t\right)^2\left(2-\mu-\mu_J^t\right)^2}{8+\left(1-\mu\right)^2+\left(1-\mu_J^t\right)^2}\right] \end{array}\right] \tag{8}$$

Where J can be represented as total neurons in the hidden layer, β1 can be described as the penalty of sparsity, β can be described as the penalty function, y_I^t can be described as a target parameter, l_2 can be described as a regularization factor (Zhang *et al.*, 2021), Y_J^P can be described as a predicted parameter and m can be described as training data. In the CNN, the hyperparameters are selected with the assistance of ROA.

3.3. Remora optimization algorithm

Remora is intelligent for its capability to swim on whales or different oceangoing hulls or marine animals. The characteristics not only depend on labor-saving and freedom from the enemy invasion. Normally, it can be distributed in tropical waters and it moves the changes of the host in cold waters. Remora can be eaten by invertebrates or other fish. Additionally, it reaches the sea location rich in bait, away from the host, eats food, and is then attracted by the new host. Additionally, it continued to move to different sea locations. Based on the remora behavior, the problem is solved. In this projected technique, the ROA will be utilized to select optimal hyperparameters of CNN. The mathematical model of remora is explained in the below section. The main process of remora is free to travel and eat thoughtfully which is explained in this section.

3.3.1. Initialization phase

In the projected ROA technique, it can be taken as a candidate solution, and the position of remora can be considered as the search space of the specific problem. The remora is swim in one- dimensional, two- dimensional, and three-dimensional position and their vector position changes continuously (Jia *et al.*, 2021). The present position of the remora is presented as follows,

$$r_I = \left(r_{I1,} r_{I2}, \ldots, r_{ID}\right) \tag{9}$$

Here, D can be represented as the dimension of the search space and I can be represented as the number of remoras. Additionally, the optimal solution of the ROA is presented as follows,

$$r_{Best} = \left(r_1^*, r_2^*, \ldots, r_D^*\right) \tag{10}$$

In the ROA, every candidate solution can be related to the fitness function. The fitness function is presented as follows,

$$f(r_I) = f\left(r_{I1,} r_{I2}, \ldots, r_{ID}\right) \tag{11}$$

Here, f can be described as the fitness function parameter. The optimal fitness parameter is presented as follows,

$$f(r_{Best}) = v(r_1^*, r_2^*, \ldots, r_D^*) \tag{12}$$

Additionally, the remora can be the main parameter to compute the solution and it can be scattered in the search space. Different marine ships can be tools to assist remora in updating the location and it contains the specific path for updating locations. With the consideration of tools, remora is computing the optimal location in the specific location. Additionally, two modes of operation are considered for computing the optimal position.

3.3.2. Exploration (Free travel)

SFO method

The remora is eating the swordfish, this position is defined as the updated process at a similar time. Related to the elite idea of this technique, the location update process of the formula was enhanced and achieved which is presented as follows,

$$r_i^{T+1} = r_{Best}^T - \left[RAND(0,1) * \left(\frac{r_{Best}^T + r_{RAND}^T}{2} \right) - r_{RAND}^T \right] \tag{13}$$

Where, r_{RAND} can be described as the random location, *t* can be described as the maximum number of iterations and *T* can be described as the number of present iterations. Elite chose remora's optimal location to enhance the update process. Additionally, the random choice of remora can be added to empower the exploration of search space. The choice of remora for various hosts is mainly related to eaten prey or not if the fitness function parameter achieved at present is higher than that of the old generation. The present fitness function parameter can be achieved with the consideration of experience attack.

3.3.3. Experience attack

To identify the experience attack, it can be required to change the host, the tuyu requirements to simultaneously develop a small step around the host, same towards the accumulation of experience. Based on the above ideas can be designed, the formulation is presented as follows,

$$r_{ATT} = r_i^T + (r_i^T - r_{PRE}) * RAND \tag{14}$$

Here, r_{ATT} can be described as a tentative step, r_{PRE} can be described as the position of the old generation. Additionally, the remora generates the active step, it is described as a small global movement. So, the *RAND* is selected. This technique is considered predictable during an efficient jump out of the local optimum and it is introduced in a large period of enhancement. After this process, the step judgment can be required after that, remora randomly select if to change the host or not. In the evaluation of this phase, the technique is explained as the comparison among the current solution and fitness function and attempted solution. Here, solving the minimum issue as an example, the fitness function parameter achieved with the consideration of the attempted solution can be lower than the present solution,

$$f(r_i^T) > f(r_{ATT})c \tag{15}$$

After that, the remora is chosen as various feeding techniques for local optimization that can be presented in the upcoming section. If the fitness parameter of the attempted variable is higher than the present solution after the host is chosen.

$$f(r_i^T) < f(r_{ATT}) \tag{16}$$

3.3.4. Exploitation (Eat thoughtfully)

WOA technique

Based on the conventional WOA technique, the remora updating process of remora position to the whale can be extracted which is presented as follows (Almotairi and Abualigah, 2020),

$$r_{i+1} = d * E^{\alpha} * COS(2\pi) + r_i \tag{17}$$

$$\alpha = RAND(0,1) * (a-1) + 1 \tag{18}$$

$$a = -\left(1 + \frac{T}{t}\right) \tag{19}$$

$$d = |r_{best} - r_i| \tag{20}$$

In a higher solution space, the remora is considered a whale, and this position is related to the same position. Here, α can be described as the random number in [-1,1] and it's presented linearly given [-2, -1] and *d* can be described as the distance between hunter and prey. The flowchart of the proposed technique is presented in Figure 2.

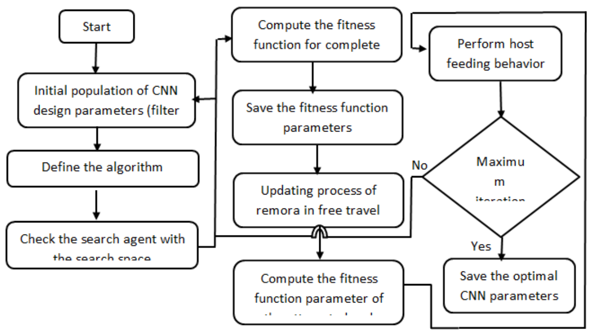

Figure 2. Flowchart of the proposed technique

Host feeding

Host feeding can be a subdivision in the exploitation procedure. In this step, the solution space is decreased to the host location space in the host. Moving on or hosting around is a thought of a small stage, this is formulated as follows,

$$r_i^T = r_i^T + a \tag{21}$$

$$a = b * (r_i^T - c * r_{best}) \tag{22}$$

$$b = 2 * v * RAND(0,1) - v \tag{23}$$

$$v = 2 * \left[1 - \frac{T}{MAX_{Iteration}} \right] \tag{24}$$

Where A can be utilized to describe a small step of movement that can be related to the volume space of remora and host. To the location of the remora and host, the remora can be a solution space and the remora factor C can be utilized to narrow the remora position. The volume of the host is 1 and the volume of the remora is selected as the host fraction.

Algorithm 1. Pseudocode of ROA

Initialize the hyperparameter of CNN, location, and memory location
Initialize the optimal fitness and optimal solution
While T<MAX iteration do
Compute the fitness parameter of each remora
Check the search agent with the search space
Update a,V
For every remora can be indexed by I do
If h(I) = 0 then
using equation (9) to update the whale position
Elseif h(I) = 1 then
Using equation (4) to position the update of attached sailfishes
Endif
Make one-step identification by equation (1)
Compute the parameter of h(I) by equation (2) (3) to judge if host changes are required
If the host is not changed, equation (5) can be utilized as the host feeding mode of remora
End for
End while

Table 1. Simulation Parameters

S. No	Description	Parameters
1	Softmax	(10,1)
2	fully connected layer 4	(84,1)
3	fully connected layer 3	(120,1)
4	Pooling layer 1	(5,5,16)
5	Convolutional layer 2	(10,10,16)
6	Pooling layer 2	(14,4,8)
7	Convolutional layer	(28,28,8)
8	Input layer	(32,32,3)
9	Number of populations	100
10	Number of iterations	100

4. Performance evaluation

The evaluation of the projected approach is presented in this section. This proposed technique is utilized for the prediction of land cover and land use in Tiruppur Tamilnadu. The projected technique is implemented in MATLAB and performances are evaluated based on performance metrics like accuracy, precision, specificity, recall, F_Measure, and Kappa. To justify the performance of the projected technique, it is compared with conventional techniques such as CNN, Markov chain and RNN, SVM. The proposed method implementation variables are given in Table 1.

4.1. Dataset description

The dataset is collected from the open-source system. These databases are containing different seven classes such as barren land, rural, fallow land, waterbody, urban, forest, and agriculture. These databases are divided into two parts training and testing phases. During the training phase, 80% of data is considered for training the network. Additionally, the remaining 20% of data is considered for testing the network. The parameters of the seven classes are presented in Tables 2 and 3. Some of the input images are illustrated in Figure 3.

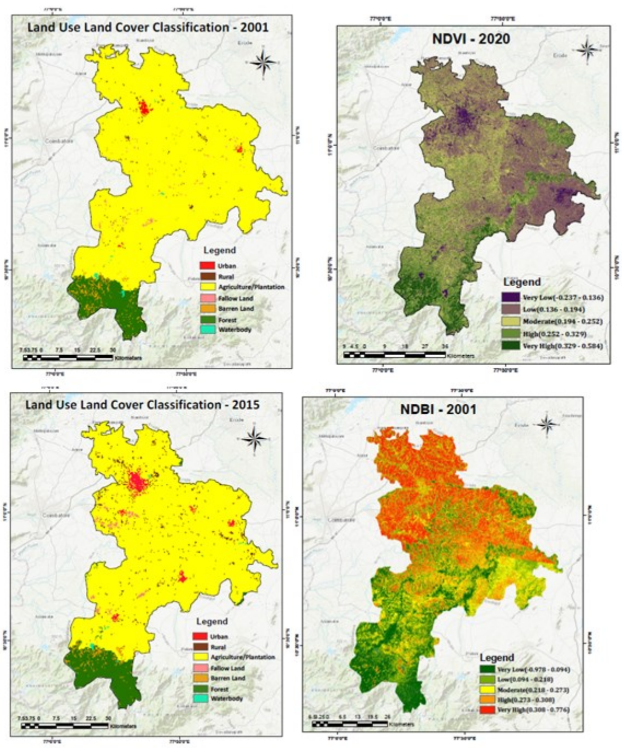

Figure 3. Sample input images

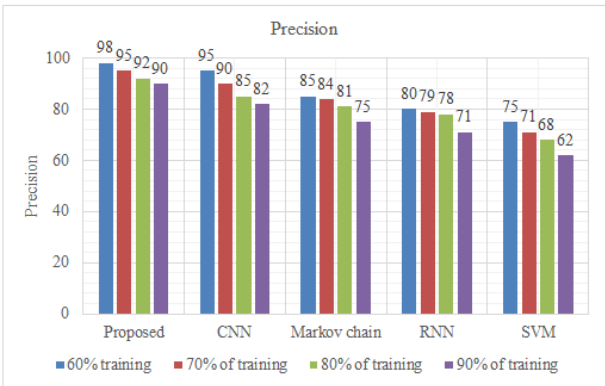

Figure 4. Precision

The projected approach is validated with the basis of the precision measure. Figure 4 The projected approach is analyzed with different training percentages such as 60% of training, 70% of training, 80% of training, and 90% of training. The projected approach is compared with conventional techniques such as CNN, Markov chain, RNN, and SVM. During 60% of the training, the proposed technique attained 98% of precision. The CNN attained 95% of precision. The Markov chain attained 85% of precision. The RNN attained 80% of precision. The SVM attained 75% of precision. Related to the validation, the projected approach achieved efficient classification precision. Similarly, the remaining training percentage also, the projected technique attained the optimal outcomes in measure of precision.

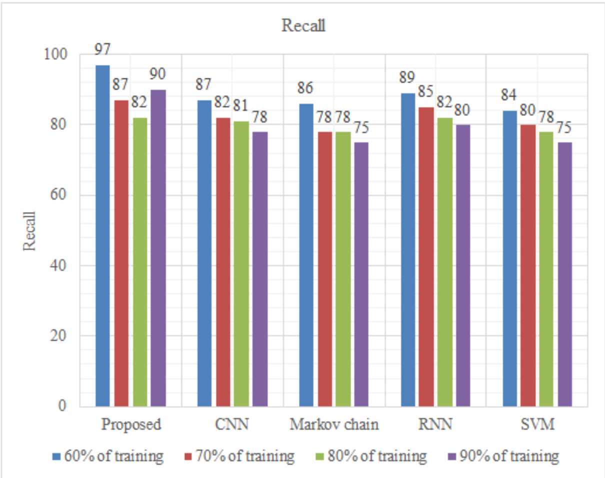

Figure 5. Recall

The projected approach is validated with the basis of the recall measure. Figure 5 The projected approach is analyzed with different training percentages such as 60% of training, 70% of training, 80% of training, and 90% of training. The projected approach is compared with conventional techniques such as CNN, Markov chain, RNN, and SVM. During 60% of the training, the proposed technique attained 97% of recall. CNN attained 87% of recall. The Markov chain attained 86% of recall. The RNN attained 89% of recall. The SVM attained 84% of recall. Related to the validation, the projected approach achieved efficient classification recall. Similarly, the remaining training percentage also, the projected technique attained the optimal outcomes in the measure of recall.

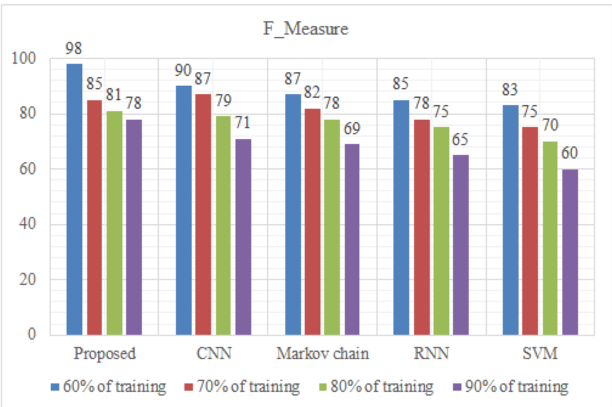

Figure 6. F_Measure

The projected approach is validated with the basis of the F_Measure measure. Figure 6 The projected approach is analyzed with different training percentages such as 60% of training, 70% of training, 80% of training, and 90% of training. The projected approach is compared with conventional techniques such as CNN, Markov chain, RNN, and SVM. During 60% of the training, the proposed technique attained 98% of F_Measure. The CNN attained 90% of F_Measure. The Markov chain attained 87% of F_Measure. The RNN attained 85% of F_Measure. The SVM attained 83% of F_Measure. Related to the validation, the projected approach achieved the efficient classification F_Measure. Similarly, the remaining training percentage also, the projected technique attained the optimal outcomes in measure of F_Measure.

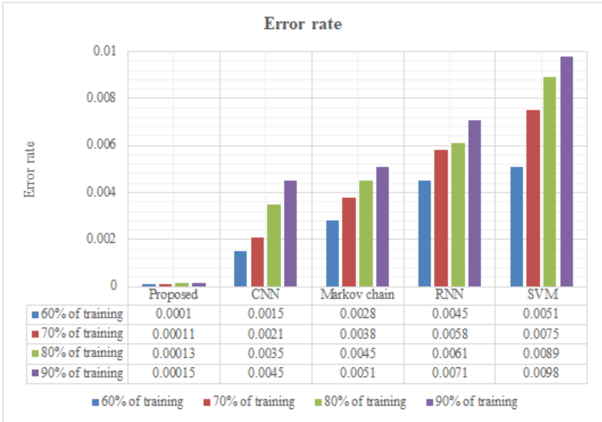

Figure 7. Error rate

The projected approach is validated based on the error rate measure. Figure 7 The projected approach is analyzed with different training percentages such as 60% of training, 70% of training, 80% of training, and 90% of training. The projected approach is compared with conventional techniques such as CNN, Markov chain, RNN, and SVM. During 60% of the training, the proposed technique attained a 0.0001 error rate. The CNN attained the 0.0015 error rate. The Markov chain attained the 0.0028 error rate. The RNN attained the 0.0045 error rate. The SVM attained the 0.0051 error rate. Related to the validation, the projected approach achieved an efficient classification error rate. Similarly, the remaining training percentage also, the projected technique attained the optimal outcomes in measure of error rate.

The projected approach is validated with the basis of the kappa measure. Figure 8 The projected approach is analyzed with different training percentages such as 60% of training, 70% of training, 80% of training, and 90% of training. The projected approach is compared with conventional techniques such as CNN, Markov chain, RNN, and SVM. During 60% of the training, the proposed technique attained 0.351 kappas. CNN attained 0.481 kappas. The Markov chain attained 0.514 kappa. The RNN attained 0.615 of kappa. The SVM attained 0.702 of kappa. Related to the validation, the projected approach achieved the efficient classification of kappa. Similarly, the remaining training percentage also, the projected technique attained the optimal outcomes in measure of kappa.

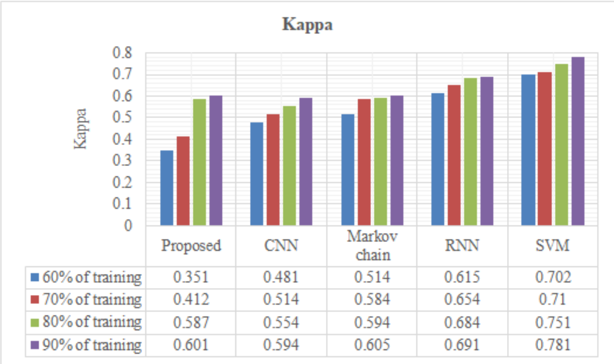

Figure 8. kappa

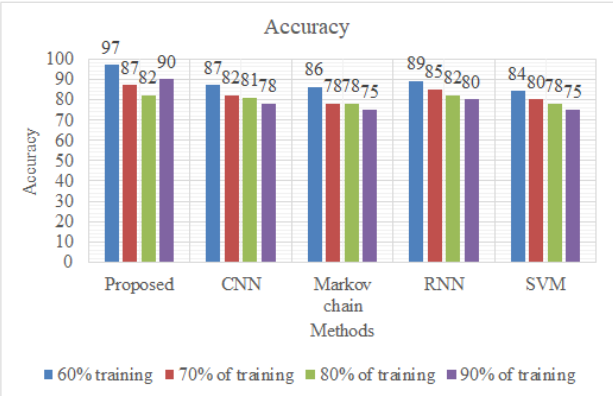

Figure 9. Accuracy

The projected approach is validated based on the accuracy measure. Figure 9 The projected approach is analyzed with different training percentages such as 60% of training, 70% of training, 80% of training, and 90% of training. The projected approach is compared with conventional techniques such as CNN, Markov chain, RNN, and SVM. During 60% of the training, the proposed technique attained 97% of accuracy. The CNN attained 87% of accuracy. The Markov chain attained 86% of accuracy. The RNN attained 89% of accuracy. The SVM attained 84% of accuracy. Related to the validation, the projected approach achieved efficient classification accuracy. Similarly, the remaining training percentage also, the projected technique attained the optimal outcomes in measure of accuracy.

The projected approach is validated based on the sensitivity measure. Figure 10 The projected approach is analyzed with different training percentages such as 60% of training, 70% of training, 80% of training, and 90% of training. The projected approach is compared with conventional techniques such as CNN, Markov chain, RNN, and SVM. During 60% of the training, the proposed technique attained 95% of sensitivity. The CNN attained 84% of sensitivity. The Markov chain attained 85% of sensitivity. The RNN attained 88% of sensitivity. The SVM attained 83% of sensitivity. Related to the validation, the projected approach achieved efficient classification sensitivity. Similarly, the remaining training percentage also, the projected technique attained the optimal outcomes in measure of sensitivity.

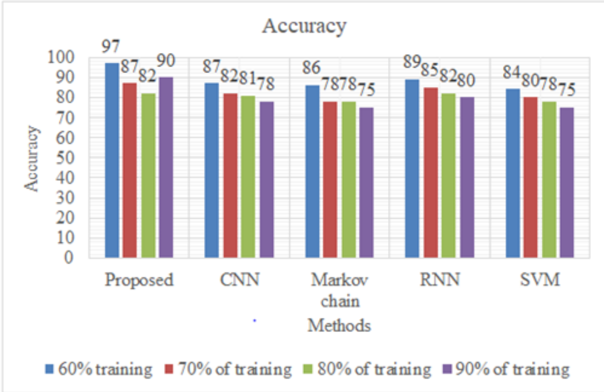

Figure 10. Sensitivity

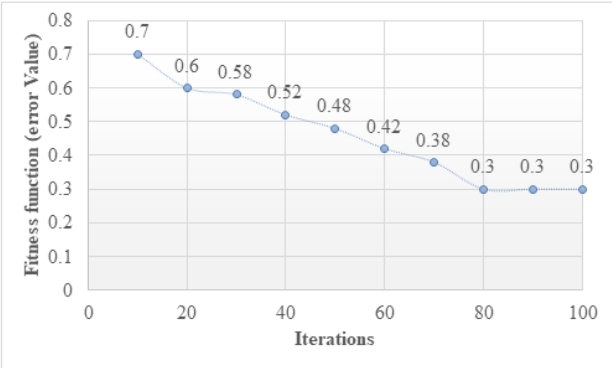

Figure 11. convergence analysis

In the projected approach, the error value is considered as the fitness function. Figure 11. The optimization technique is to select the optimal CNN parameter with the basis of error rate. Related to the analysis, the projected technique attained the optimal outcomes in land use and land cover classification.

The results of this study show that the proposed approach, referred to as the projected approach, performs well in terms of precision, recall, F-measure, error rate, and kappa measures when compared to conventional techniques such as CNN, Markov chain, RNN, and SVM. When the projected approach is trained on 60% of the data, it achieves a precision of 98%, recall of 97%, F-measure of 98%, an error rate of 0.0001, and kappa of 0.351. These results are significantly better than those achieved by the other techniques. As the amount of training data increases to 70%, 80%, and 90%, the projected approach continues to outperform the other techniques in all measures. Overall, these results suggest that the projected approach is an effective method for classification tasks.

5. Conclusion

This paper has developed HCNN for land use and land cover changes prediction in Tiruppur Tamilnadu. Initially, the databases are collected from the open-source system. And the image dataset has been pre-processed using the image augmentation technique. Through which the image has been resized and processed for training with the proposed mode. The resized images are sent to the HCNN for prediction of land cover and land use changes in Tiruppur Tamilnadu. The proposed classifier is a combination of CNN and ROA. In the CNN, the ROA is utilized to select the hyperparameters to enable efficient prediction in land use and land cover changes. The proposed classifier is implemented in MATLAB and performances are evaluated by performance metrics such as accuracy, precision, recall, sensitivity, F_Measure, and Kappa. The proposed methodology is compared with conventional techniques such as CNN, Markov chain model, and RNN respectively. Based on the analysis, the projected approach attained the best outcomes in terms of performance metrics.

The proposed Hybrid Convolutional Neural Network (HCNN) methodology outperforms the conventional techniques such as the CNN, Markov chain model, RNN, and SVM in terms of several evaluation measures including precision, recall, F-measure, error rate, and kappa. In particular, the HCNN appears to consistently achieve higher scores than the other techniques across all training percentages and evaluation measures.

Table 2. Parameters of the seven classes

Class Name	Barren Land	Rural	Fallow Land	Waterbody	Urban	Forest	Agriculture
Barren Land	0.0626	0.0214	0.0033	0.0012	0.0041	0.3971	0.5104
Rural	0.0006	0.1149	0.0043	0.0070	0.2772	0.0005	0.5955
Fallow Land	0.0010	0.0868	0.0065	0.0015	0.0333	0.0011	0.8698
Waterbody	0.0003	0.0198	0.0010	0.6474	0.0027	0.0061	0.3227
Urban	0.0000	0.0022	0.0002	0.0000	0.9309	0.0000	0.0666
Forest	0.0646	0.0057	0.0005	0.0045	0.0009	0.7555	0.1683
Agriculture	0.0011	0.0515	0.0068	0.0010	0.0274	0.0026	0.9094

Table 3. Notation table

S.No.	Symbols and acronyms	Definition and abbreviations
1	LU/LC	Land use and land cover change
2	HCNN	Hybrid Convolutional Neural Network
3	ROA	Remora Optimization Algorithm
4	GEE	Google Earth Engine
5	CL_F^S	pixel parameter and filter position of the convolution layer
6	Pat_H and Pat_W	Patch height and width
7	Feat_K	feature vector, *K* is the total input features
8	$w_{k,j}^{FC}$	weight of input feature of hidden layer
9	J	total neurons in the hidden layer
10	β1	penalty of sparsity
11	β	penalty function
12	y_I^t and Y_J^P	Target and predicted parameters
13	r_{RAND}	random location

Declaration:

Ethics Approval and Consent to Participate:

No participation of humans takes place in this implementation process

Human and Animal Rights

No violation of Human and Animal Rights is involved.

Funding

No funding is involved in this work.

Conflict of Interest

Conflict of Interest is not applicable in this work.

Authorship contributions

There is no authorship contribution

Acknowledgment

There is no acknowledgment involved in this work.

References

Abijith D. and Saravanan S. (2021). Assessment of land use and land cover change detection and prediction using remote sensing and CA Markov in the northern coastal districts of Tamil Nadu, India. *Environmental Science and Pollution Research,* 1–13.

Almotairi K.H. and Abualigah L. (2022). Hybrid reptile search algorithm and remora optimization algorithm for optimization tasks and data clustering. *Symmetry,* **14**(3), 458.

Berihun M.L., Tsunekawa A., Haregeweyn N., Meshesha D.T., Adgo E., Tsubo M., Masunaga T., Fenta A.A, Sultan D. and Yibeltal M. (2019). Exploring land use/land cover changes, drivers and their implications in contrasting agroecological environments of Ethiopia. *Land Use Policy*, **87**, 104052.

Cegielska K., Noszczyk T., Kukulska A., Szylar M., Hernik J., Dixon-Gough R., Jombach S., Valánszki I. and Kovács K.F. (2018). Land use and land cover changes in post-socialist countries: Some observations from Hungary and Poland. *Land use policy*, **78**, 1–18.

Choudhury D., Das K. and Das A. (2019). Assessment of land use land cover changes and its impact on variations of land surface temperature in Asansol-Durgapur Development Region. *The Egyptian Journal of Remote Sensing and Space Science,* **22**(2), 203–218.

Geng J., Shen S., Cheng C. and Dai K. (2022). A hybrid spatiotemporal convolution-based cellular automata model (ST-CA) for land-use/cover change simulation. *International*

Journal of Applied Earth Observation and Geoinformation, **110**, 102789.

Girma R., Fürst C. and Moges A. (2022). Land use land cover change modeling by integrating the artificial neural network with cellular Automata-Markov chain model in the Gidabo river basin, main Ethiopian rift. *Environmental Challenges*, **6**, 100419.

Hakim A.M.Y., Baja S., Rampisela D.A. and Arif S. (2021). Modelling land use/land cover changes prediction using multi-layer perceptron neural network (MLPNN): a case study in Makassar City, Indonesia. *International Journal of Environmental Studies,* **78**(2), 301–318.

Hamad R., Balzter H. and Kolo K. (2018). Predicting land use/land cover changes using a CA-Markov model under two different scenarios. *Sustainability,* **10**(10), 3421.

Hussain S., Mubeen M., Ahmad A., Akram W., Hammad H.M., Ali M., Masood N., *et al.* (2020). Using GIS tools to detect the land use/land cover changes during forty years in Lodhran district of Pakistan. *Environmental Science and Pollution Research,* **27**(32), 39676–39692.

Jagannathan J. and Divya C. (2021). Deep learning for the prediction and classification of land use and land cover changes using deep convolutional neural network. *Ecological Informatics,* **65**, 101412

Jia H., Peng X. and Lang C. (2021). Remora optimization algorithm. *Expert Systems with Applications,* **185**, 115665.

Khamchiangta D. and Dhakal S. (2020). Time series analysis of land use and land cover changes related to urban heat island intensity: Case of Bangkok Metropolitan Area in Thailand. *Journal of Urban Management,* **9**(4), 383–395.

Kumar A., Vashishtha G., Gandhi C.P., Zhou Y., Glowacz A., and Xiang J. (2021). Novel convolutional neural network (NCNN) for the diagnosis of bearing defects in rotary machinery. *IEEE Transactions on Instrumentation and Measurement,* **70**, 1–10.

Mansour S., Al-Belushi M. and Al-Awadhi T. (2020). Monitoring land use and land cover changes in the mountainous cities of Oman using GIS and CA-Markov modeling techniques. *Land Use Policy,* **91**, 104414.

Namugize J.N., Jewitt G. and Graham M. (2018). Effects of land use and land cover changes on water quality in the uMngeni river catchment, South Africa. *Physics and Chemistry of the Earth, Parts a/b/c,* **105**, 247–264.

Naushad R., Kaur T. and Ghaderpour E. (2021). Deep Transfer Learning for Land Use and Land Cover Classification: A Comparative Study. *Sensors,* **21**(23), 8083.

Nayak S. and Mandal M. (2019). Impact of land use and land cover changes on temperature trends over India. *Land Use Policy,* **89**, 104238.

Souza C.M., Z Shimbo J., Rosa M.R., Parente L.L., Alencar A.A., Rudorff B.F., Hasenack H., *et al.* (2020). Reconstructing three decades of land use and land cover changes in Brazilian biomes with Landsat archive and earth engine. *Remote Sensing,* **12**(17), 2735.

Tegegne A M. (2022). Applications of Convolutional Neural Network for Classification of Land Cover and Groundwater Potentiality Zones.

Vinayak B., Lee H.S. and Gedem S. (2021). Prediction of land use and land cover changes in Mumbai City, India, using remote sensing data and a multilayer perceptron neural network-based Markov chain model. *Sustainability,* **13**(2), 471.

Xu X., Shrestha S., Gilani H., Gumma M.K., Siddiqui B.N. and Jain A.K. (2020). Dynamics and drivers of land use and land cover changes in Bangladesh. *Regional Environmental Change,* **20**(2), 1–11.

Zhang Y.D., Satapathy S.C., Guttery D.S., Górriz J.M. and Wang S.H. (2021). Improved breast cancer classification through combining graph convolutional network and convolutional neural network. *Information Processing & Management,* **58**(2), 102439.